Lab on a Chip

PAPER

View Article Online
View Journal | View Issue

Phaseguides as tunable passive microvalves for liquid routing in complex microfluidic networks†

Cite this: *Lab Chip*, 2014, **14**, 3334

Ender Yildirim,‡[ab] Sebastiaan J. Trietsch,‡[ac] Jos Joore,[c] Albert van den Berg,[d] Thomas Hankemeier[a] and Paul Vulto*[ac]

Received 28th February 2014,
Accepted 17th June 2014

DOI: 10.1039/c4lc00261j

www.rsc.org/loc

A microfluidic passive valving platform is introduced that has full control over the stability of each valve. The concept is based on phaseguides, which are small ridges at the bottom of a channel acting as pinning barriers. It is shown that the angle between the phaseguide and the channel sidewall is a measure of the stability of the phaseguide. The relationship between the phaseguide–wall angle and the stability is characterized numerically, analytically and experimentally. Liquid routing is enabled by using multiple phaseguide with different stability values. This is demonstrated by filling complex chamber matrices. As an ultimate demonstration of control, a 400-chamber network is used as a pixel array. It is the first time that differential stability is demonstrated in the realm of passive valving. It ultimately enables microfluidic devices for massive data generation in a low-cost disposable format.

Introduction

Passive valves have been a major focal point in microfluidics since the emergence of the field in the '90s.[1–4] Passive valves hold the promise to control routing of liquids in complex microfluidic channel networks without the use of moving parts or complex actuation schemes. The idea that microfluidic functionality could be "preprogrammed" in the device, rather than using *ad hoc* control over valve states, is alluring. It would eliminate the need for user interference and/or bulky control equipment. It also holds the promise of cheaper fabrication than active valving platforms. Passive valve-based microfluidic systems are therefore the most amenable to make microfluidics available as a low-cost laboratory disposable.

Passive valves can be largely subdivided into two types: hydrophobic barriers and pinning barriers. The first type is typically created by patterning a hydrophobic material such as Teflon, parylene or self-assembled monolayers on one or more of the channel walls.[5,6] Given that the wettability of a channel suddenly changes from hydrophilic to hydrophobic, additional energy is required to breach the barrier. The pressure required for breaching such valves is typically higher than that for pinning barriers.

The mechanisms behind pinning barriers are less intuitive to understand. Retarding effects due to pinning are sometimes erroneously explained as occurring due to hydrodynamic resistance of channels. Pinning effects occur due to a change in geometry, such that advancement of a liquid–air meniscus causes an increase in its principal radii of curvature to such an extent that this would require an increased applied external pressure. Impressive examples of pinning barriers were shown by Zimmermann *et al.*, Melin *et al.* and Ahn *et al.*[7–9]

Alternatives to passive valve-based systems are autonomous capillary systems that use capillarity as a driving force and/or control hydrodynamic resistance of channels for liquid routing.[10,11]

However, none of these systems could achieve a level of complexity that is achieved by active valving systems such as PDMS microvalves[12,13] or electrowetting platforms.[14] The aspect that is lacking so far is differential control over the stability of passive valves. For complex geometries, valves should be breached in a certain, preprogrammed order. For this, precise control over the stability of each valve is necessary. So far, however, differential stability has not been demonstrated in the realm of passive valves.

We introduced the concept of "phaseguides" almost a decade ago.[15] Phaseguides are a type of pinning barriers that allow controlled filling and emptying of microfluidic chambers of any shape. Phaseguide-based microfluidic systems have gained widespread use over the recent years, leading to applications in 3D cell culturing, RNA extraction, recombinase

[a] *Division for Analytical Biosciences, Leiden Academic Centre for Drug Research, University of Leiden, 2300 RA, Leiden, The Netherlands. E-mail: p.vulto@lacdr.leidenuniv.nl; Tel: +31 (0)71 527 4509*
[b] *Mechanical Engineering Department, Cankaya University, 06810, Ankara, Turkey*
[c] *MIMETAS BV, P.O. Box 11002, 2301 EA, Leiden, The Netherlands*
[d] *MESA+ Institute for Nanotechnology, University of Twente, 7500 AE, Enschede, The Netherlands*

† Electronic supplementary information (ESI) available: Text explaining the analytical and simulation models. Video footage of Fig. 1f, 2b, 2g, and 3a. See DOI: 10.1039/c4lc00261j

‡ These authors contributed equally to this work.

polymerase amplification, concentration of bacteria, sandwich immunoassays, electroextraction and magnetic bead-based assays.[16–24] In ref. 25 we suggested that phaseguides would ultimately enable complex liquid routing schemes.

Here we show for the first time that the stability of passive valves in general and phaseguides in particular could be differentially controlled. The burst pressure of the phaseguide was precisely controlled by varying the angle between the phaseguide and the wall. A smaller phaseguide–wall angle leads to a lower burst pressure, while a larger angle leads to an increased stability of the phaseguide. This concept was applied to create pinning barriers with differential stability and utilized to fill complex arrays of chambers in one pipetting step only. As a demonstration of selectivity we show a 400-chamber array in which we selectively fill the chamber while leaving the others empty to ultimately 'write' the word μTAS.

Results

Phaseguide stability

In this work, a phaseguide is patterned as a shallow barrier at the bottom of the microfluidic channel (Fig. 1a). An advancing liquid meniscus first aligns along the phaseguide and then overflows it at its weakest point if sufficient pressure is built up across the meniscus.[25] This weakest point is typically the smallest angle along the phaseguide (phaseguide–wall angle α in Fig. 1a). This is typically the angle between the phaseguide and an intersecting sidewall. Control over this angle implies control over the stability of the phaseguide.

To assess the relationship between phaseguide stability and the angle between the phaseguide and a sidewall, a simulation was performed using Surface Evolver (a software package developed to examine interfaces under surface

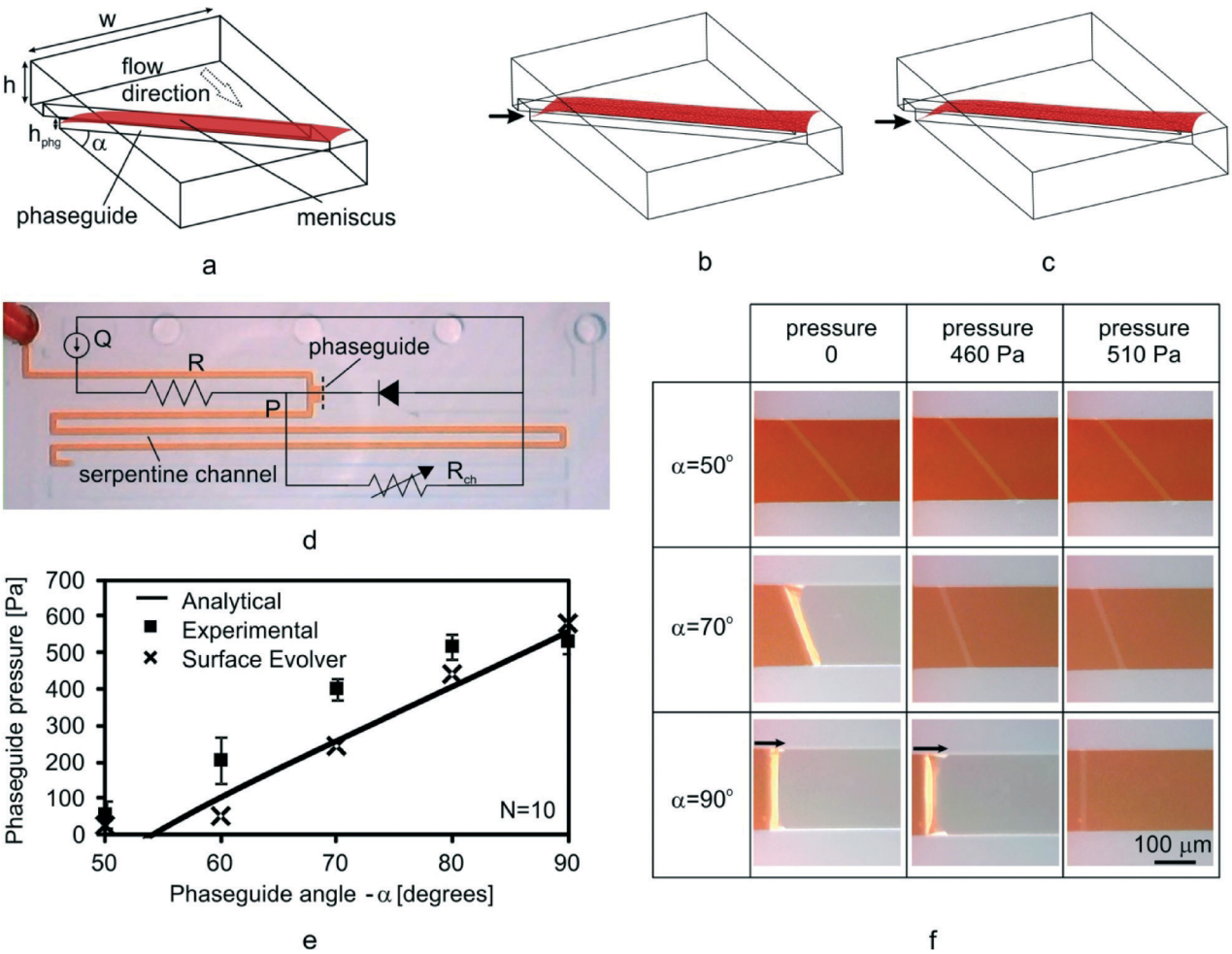

Fig. 1 Quantification of the phaseguide stability as a function of the phaseguide wall angle (a) schematic of the liquid air meniscus that is pinned on a phaseguide (b, c) snapshots of the Surface Evolver simulation showing meniscus advancement at the location of the smallest angle, α (depicted by the arrow); overflow occurs when the tip of the meniscus touches the channel bottom. (d) test structure used to experimentally determine the phaseguide pressure by equivalent electrical circuit analogy; (e) quantification of phaseguide stability as a function of the angle by experimental, numerical and analytical methods. All three methods show a clear increase in phaseguide stability with increasing phaseguide–wall angle. Below a certain angle the phaseguide loses its barrier function, which is designated the critical angle. Error bars indicate the standard error with n = 10 observations. See ESI† for experimental and simulation results. (f) frames captured at different pressures for three different phaseguide–wall angles during one set of experiments. For α = 50° no alignment was observed. Arrows indicate the stretching of the meniscus before overflow. See ESI† for Video S1.

tension,[26] see Fig. 1b–c). The simulation shows that the meniscus moves downwards along the sidewall of the phaseguide. We define the overflow of the phaseguide as the point where the barrier function is relieved, *i.e.* when the meniscus touches the bottom substrate.

In addition to the simulation, we developed an analytical model to estimate the principal radii of curvature of the meniscus. The Laplace pressure developed across the meniscus at the instant of overflow, given by the Young–Laplace equation (eqn (1)), is defined as the phaseguide pressure (P_{phg}) and used as a measure of phaseguide stability.

$$P_{phg} = \gamma\left(\frac{1}{R_1} + \frac{1}{R_2}\right) \quad (1)$$

Here, γ is the surface energy of the liquid and R_1 and R_2 represent the principle radii of curvature of the meniscus at the instant of overflow. R_1 and R_2 could be derived from the various contact angles and geometrical aspects (see the ESI† text for details).

To validate the analytical model and simulation results, we fabricated test structures (Fig. 1d) including phaseguides with phaseguide–wall angles varying from 50 to 90 degrees. The phaseguides were positioned adjacently to a meandering channel close to the fluid inlet. Application of a constant flow rate resulted in gradual filling of the meander, thereby increasing the hydrodynamic resistance and thus the back pressure over the meniscus that is pinned on the phaseguide. By electrical analogy (Fig. 1d), this backpressure (P) can be calculated as

$$P = R_{ch}Q \quad (2)$$

with constant flow (Q) and channel resistance, R_{ch}, that increases with the length of the sepentine channel wetted by the liquid. The back pressure at the instant of overflow was recorded as the phaseguide pressure. Contact angles of the phaseguide and the channel wall material were assumed to be 70°, while top and bottom substrate contact angles were 20°. Channel height, phaseguide height, and channel width were set to 120 μm, 30 μm, and 200 μm, respectively. Fig. 1e compares the analytical model and the simulation results with the experimental results. There is a close correlation between the analytical model and the simulation model. The experimental results show slightly higher phaseguide pressures than predicted by the analytical and numerical models. The trend, however, is comparable to these models. We assume this is due to the fact that the corner between the phaseguide and the side wall is not infinitely sharp as well as to a deviation in the contact angle with respect to measured values.

Both analytical and simulated models show that below a certain angle, the phaseguide immediately overflows without meniscus alignment. This is in accordance with the observation of Concus and Finn, who stated that a liquid under surface tension would wet a wedge with an angle less than a critical value.[27] This critical angle can be found as ($180° - \theta_1 - \theta_2$), where θ_1 and θ_2 are the contact angles of water on the phaseguide and the wall material, respectively. The critical angle was also found experimentally. In 6 out of 10 observations for 50 degree phaseguides, the liquid immediately overflowed the phaseguide without alignment (see ESI† Video S1). The fact that the meniscus alignment does not occur indicates the absence of a barrier function. This result implies a phaseguide pressure of less than or equal to zero. Since the test structure (Fig. 1d) does not allow measuring negative phaseguide pressures, we defined the phaseguide pressure as zero for these cases. For a material contact angle of 70°, the Concus–Finn theorem yields a critical angle of 40°. The discrepancy with the modeled and experimental values might be due to a range of causes, including meniscus stretching, corner flow effects and the fact that the angles are not infinitely sharp.

Complex liquid routing

Differential stability of the phaseguides implies that upon pinning of a meniscus on multiple phaseguides, the phaseguide with the lowest stability will overflow first[25] (Fig. 2a). To demonstrate this concept for liquid routing, we designed a microfluidic network composed of 14 parallel chambers placed as rungs between common inlet and outlet channels (Fig. 2b). The design is such that the hydrodynamic resistance between the inlet and the outlet measured across any of the chambers is the same. For bubble-free routing of liquid through this network, overflow must occur at the outlet of the first chamber only after all the chambers are filled. This was achieved by placing relatively stable phaseguides (phaseguide #3 in Fig. 2b) at the outlets of chambers 2–14, while placing a less stable phaseguide (phaseguide #2 in Fig. 2b) at the outlet of chamber 1. Phaseguide #2 must be stable enough to prevent a premature overflow due to the increasing back pressure during the filling process. To satisfy these criteria, phaseguide #3 was designed as a curve protruding into the outlet channel such that the phaseguide–wall angle is 150°. Phaseguide #2 was designed as a straight line making a 90° angle with the channel wall. In addition to these phaseguides, curved phaseguide #1 was utilized at the inlet of chambers 1–13 to ensure sequential filling of the chambers. These phaseguides were designed as a smooth curve having a 30 degree angle with the chamber wall. Fig. 2d shows a detail of the filling process. The complex shaped phaseguides at the inlets ensure that overflow occurs only after the meniscus has advanced into the chamber. The relatively stable phaseguides at the chamber outlets keep the relating menisci pinned, while another meniscus proceeds in the downstream direction for filling the remaining chambers. As the meniscus reaches the last chamber (see Fig. 2e), overflow of phaseguide #2 occurs. The meniscus advances through the outlet channel and sequentially merges with the menisci pinned at the stable #3 phaseguides. The result is that the complete network is filled without any air entrapped in the channels or chambers (Fig. 2f).

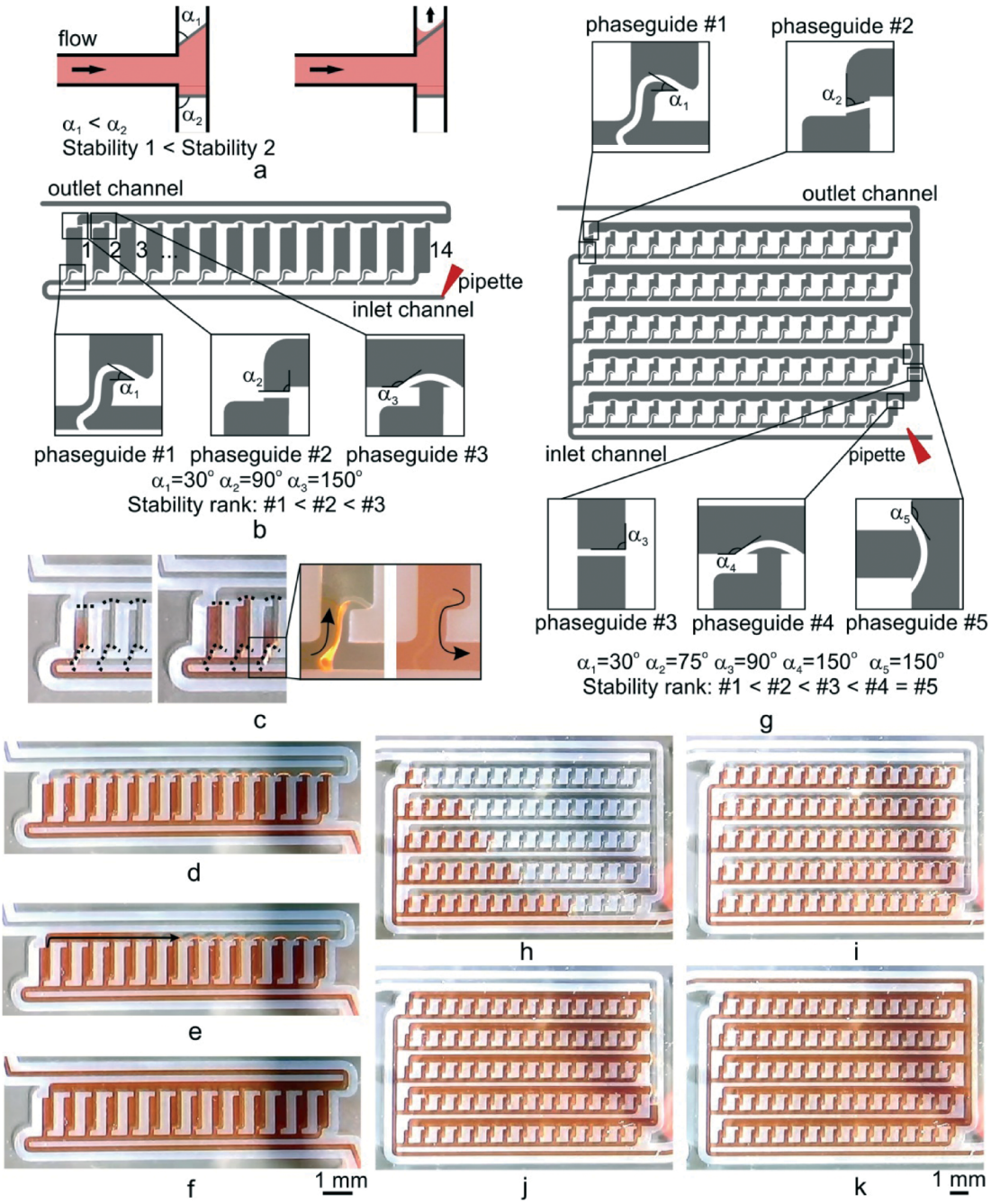

Fig. 2 Liquid routing through differential phaseguiding: (a) concept of differential phaseguiding: a liquid that is pinned on multiple phaseguides will overflow the least stable phaseguide, *i.e.*, the phaseguide with the smallest phaseguide–wall angle; b) a string of 14 chambers containing phaseguides of 3 different stability values: phaseguide #1 serves to fill each chamber consecutively, phaseguide #3 is not intended to be overflowed, while phaseguide #2 is to be overflowed only after filing all 14 chambers; c) close-up of the filling sequence of the first 3 chambers; d) the channel system upon filling all 14 chambers; e) overflow of phaseguide #2; f) the channel network upon complete filling; see also the ESI† Video S2. g) Multitude of chamber rows in parallel containing phaseguides of 4 different stabilities; h–k) filling of a matrix of chambers, see also ESI† Video S3.

The density of parallel data generation can be further increased by successively placing multiples of these ladder-like structures in parallel. This is shown in Fig. 2g–k. The figures show an array composed of 5 rows each of which comprise 15 chambers to create a total of 75 identical microfluidic chambers. In this configuration, the same phaseguide pattern is used as shown in Fig. 2a–f. In addition, 150 degree phaseguide #5 was utilized to block the outlet channel of each row at the common outlet channel. To ensure that overflow occurs at the outlet of the first row, a less stable phaseguide #3 of 90° was used here. To ensure that this 90 degree phaseguide is not overflowed before all the rows are filled,

the stability of phaseguide #2 was reduced, utilizing a 75 degree angle.

As a visual demonstration of the level of control that could be exerted using differential phaseguiding, we utilized a chamber array as a pixel array. Selective filling and non-filling of chambers due to the phaseguide shape result in the word μTAS (in reference to the micro total analysis system, the original name for Lab-on-a-Chip,[28] see Fig. 3f and ESI† Video S4). The pixel array consists of 20 hairpin loops. Each loop contains 20 microchambers connecting the upstream and downstream channels of the loop. The outlet of each chamber contains a stable phaseguide of 90°, with the exception of the last chamber of each loop that does not contain a phaseguide. Each chamber that is to be filled with liquid contains a phaseguide #1 similar to the one shown in Fig. 2. Each chamber that is meant to stay empty contains a straight phaseguide of 90° at the inlet. Fig. 3b–e show the selective filling of chambers in a single loop. Fig. 3f shows the complete array filled, depicting the word μTAS.

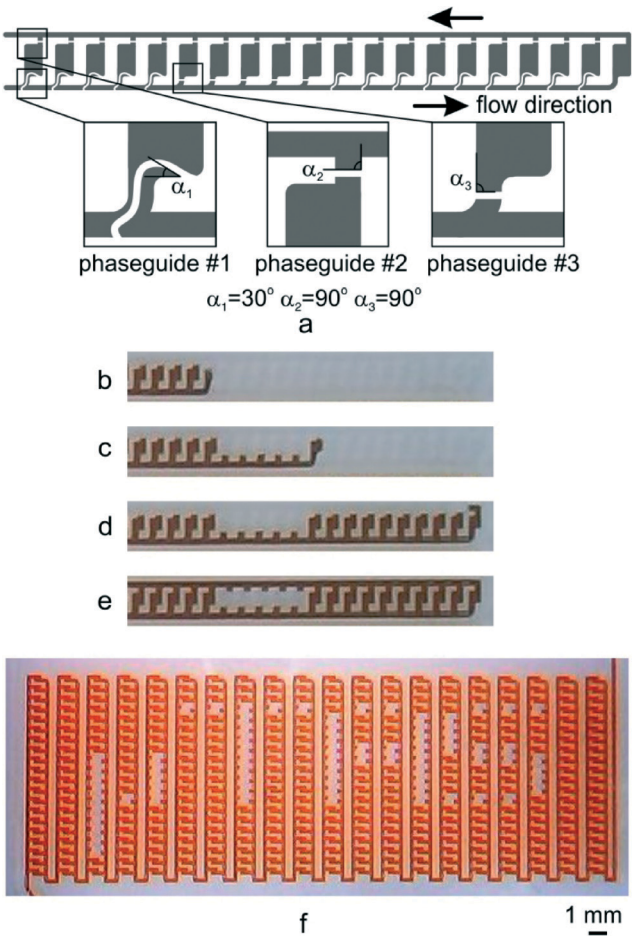

Fig. 3 Filling of a 20 × 20 pixel array: (a) one of the loops in the array containing 3 types of phaseguides. Phaseguide #1 is of lower stability than phaseguide #3 enabling selective filling of each chamber. Phaseguides #2 and #3 are not intended to be overflowed. b–e) Close up of the filling of a single loop in which 3 chambers are deliberately left empty; (f) filling of the entire pixel array displaying the word μTAS. See also the ESI,† Video S4.

Discussion

The above results, to our knowledge, are the first to demonstrate differential valving using passive pinning barriers, which was made possible by varying the angle between the phaseguide and the sidewall. However, a sharp bend in the phaseguide itself or a branching structure making a similar V-shape would also enable tuning of the stability.[25] This finding is a consequence from the insight that the pinning barrier stability is governed by both its vertical and horizontal cross-sectional shapes. Earlier literature typically describes a pinning barrier as governed by a two-dimensional cross-sectional shape.[1,29] Others did include the third dimension in their analysis, but failed to observe the importance of the V-shaped grooves at the edges of the barriers.[30] As clearly shown in the above results, it is of critical importance to take both the horizontal and vertical cross-sectional shapes into account when assessing the stability of a pinning barrier. In our case, when the pinning barrier is positioned as a ridge on the bottom of a channel, the variation of the horizontal cross-sectional shape is more interesting than that of the vertical cross-sectional shape. As most microfabrication techniques are 2.5D at best, horizontal variations of design are strongly preferable over difficult to vary vertical geometries. Variations in the horizontal plane, such as used above, are usually part of the routine design and fabrication procedures, while adjusting the shape in the vertical cross section is typically limited by the fabrication technique and cannot be varied at will.

This innovation may have important consequences for the applicability of passive valves. Whereas active valves (PDMS microvalves in particular[12]) have largely lived up to their promises to enable massively parallel operations, passive valve-based platforms have failed to do so despite their inherent advantages such as ease of fabrication, stand-alone operation and wide material compatibility. This was mainly caused by the fact that active valve-based platforms offer selective liquid progression, while this was not possible in passive valve platforms. By introducing differential stability concepts, selective liquid progression is now possible in passive systems by preprogramming the barrier stability. This enables sequentially controlled filling of the channel networks.

In this paper we demonstrated the principle of differential valving using phaseguides without referring to any particular application. An example of the potential application of the technique is in performing combinatorial assays. Recently, it was shown that phaseguides can be used to laminate static volumes of liquids in a common chamber.[20] This concept can be combined with the one-shot dispensing techniques described here in order to obtain an array of chambers filled in parallel with different combinations of reagents. Further extrapolation towards multi-layer microfluidic channel networks enables applications in combinatorial PCR, library preparation for next-generation sequencing, or single-cell analysis that are currently performed in active valving platforms.[31]

The primary interest of our research groups goes towards increasing the data density of the microfluidic 3D cell cultures or Organs-on-a-Chip.[16] These devices today suffer from the typical microfluidics paradox, where the actual active area is much smaller than the surrounding chip and equipment used for world-to-chip interfacing. Multiplexing of tissues, combinatorial screening techniques and one-shot perfusion of cell cultures would greatly assist in increasing the density of tissues on a single plate.

Experimental

Fabrication

The structures were fabricated as previously described.[25] Briefly, phaseguides and channels walls were made from dry film resist (Ordyl SY330, Elga Europe) on glass substrates using standard photolithographic techniques. The microfluidic device was covered with a glass wafer on which the inlets and outlets were created by ultrasonic drilling. Nominal heights of the channels and the phaseguides were set to 120 μm and 30 μm, respectively.

Phaseguide characterization

To determine the back pressure at the instant of overflow, we measured the length of the serpentine channel wetted by the liquid and inserted in the equation for the pressure drop (ΔP) in rectangular channels[32] (eqn (3))

$$\Delta P = \frac{12\mu QL}{h^3 w}\left(1 - 0.630\frac{h}{w}\right)^{-1} \quad (3)$$

where μ is the dynamic viscosity of the liquid, Q is the volumetric flow rate, L is the wetted length of the serpentine channel, h is the channel height, and w is the channel width. To determine the wetted length of the serpentine channel, the flow was recorded using a digital microscope. The wetted length was determined by processing the captured image at the instant of overflow using ImageJ. During the tests, the flow rate was set to 20 μl min^{-1}.

Testing of the chips

To test the microfluidic device, food-dye-colored de-ionized water was dispensed with a pipette. Pipette tips precisely fit the access holes such that they can be used for active pumping of liquids in the channels.

Conclusion

A passive liquid routing platform was introduced based on differential phaseguiding. Differential stability was achieved by variation of the angle between the phaseguide and the channel wall. Stability was quantified experimentally, numerically and analytically. A 400-pixel array could be filled in a controlled manner in one pipetting step only. Differential phaseguiding resolves a critical bottleneck in microfluidics, making it available as an affordable laboratory disposable for massive parallel data generation.

Acknowledgements

Authors like to thank Koen Sweering and Athanasios Giannitsis for fabrication of microfluidic chips. Our gratitude also goes to the Technology Foundation STW, the Netherlands Metabolomics Centre and the Scientific and Technological Research Council of Turkey for funding this research.

Notes and references

1 P. Man, C. Mastrangelo, M. Burns and D. Burke, *Proceedings of the 11th Annu. Int. Work. Micro Electro Mech. Syst.*, Heidelberg, 1998.
2 M. R. McNeely, M. K. Sputea, N. A. Tusneem and A. R. Oliphant, *J. Assoc. Lab. Autom.*, 1999, **4**, 30.
3 K. W. Oh and C. H. Ahn, *J. Micromech. Microeng.*, 2006, **16**, R13.
4 A. K. Au, H. Lai, B. R. Utela and A. Folch, *Micromachines*, 2011, **2**, 179.
5 P. Man, C. Mastrangelo, M. Burns and D. Burke, *Proceeding of Transducers*, Sendai, 1999.
6 Y. Feng, Z. Zhou, X. Ye and J. Xiong, *Sens. Actuators, A*, 2003, **108**, 138.
7 M. Zimmermann, P. Hunziker and E. Delamarche, *Microfluid. Nanofluid.*, 2008, **5**, 395.
8 J. Melin, N. Roxhed, G. Gimenez, P. Griss, W. van der Wijngaart and G. Stemme, *Sens. Actuators, B*, 2004, **100**, 463.
9 C. H. Ahn, A. Puntambekar, S. M. Lee, H. J. Cho and C. C. Hong, *Proceedings of Micro Total Anal. Syst.*, Enschede, 2000.
10 D. Juncker, H. Schmid, U. Drechsler, H. Wolf, M. Wolf, B. Michel, N. de Rooij and E. Delamarche, *Anal. Chem.*, 2002, **74**, 6139.
11 R. Safavieh and D. Juncker, *Lab Chip*, 2013, **13**, 4180.
12 M. A. Unger, H. P. Chou, T. Thorsen, A. Scherer and S. R. Quake, *Science*, 2000, **288**, 113.
13 T. Thorsen, S. J. Maerkl and S. R. Quake, *Science*, 2002, **298**, 580.
14 B. Hadwen, G. R. Broder, D. Morganti, A. Jacobs, C. Brown, J. R. Hector, Y. Kubota and H. Morgan, *Lab Chip*, 2012, **12**, 3305.
15 P. Vulto, G. Medoro, L. Altomare, G. A. Urban, M. Tartagni, R. Guerrieri and N. Manaresi, *J. Micromech. Microeng.*, 2006, **16**, 1847.
16 S. J. Trietsch, G. D. Israëls, J. Joore, T. Hankemeier and P. Vulto, *Lab Chip*, 2013, **13**, 3548.
17 J. W. Schoonen, V. Van Duinen, A. Oedit, P. Vulto, T. Hankemeier and P. W. Lindenburg, *Anal. Chem.*, 2014, DOI: 10.1021/ac500707v.
18 P. Vulto, G. Dame, U. Maier, S. Makohliso, S. Podszun, P. Zahn and G. A. Urban, *Lab Chip*, 2010, **10**, 610.
19 R. Gottheil, N. Baur, H. Becker, G. Link, D. Maier, N. Schneiderhan-Marra and M. Stelzle, *Biomed. Microdevices*, 2013, **16**, 163.

20 C. Phurimsak, E. Yildirim, M. D. Tarn, S. J. Trietsch, T. Hankemeier, N. Pamme and P. Vulto, *Lab Chip*, 2014, **14**, 2334.
21 C. Y. Chen, T. C. Chiang, C. M. Lin, S. S. Lin, D. S. Jong, F. S. Tsai, J. T. Hsieh and A. M. Wo, *Analyst*, 2013, **138**, 4967.
22 D. Puchberger-Enengl, C. Krutzler, F. Keplinger and M. J. Vellekoop, *Lab Chip*, 2014, **14**, 378.
23 C. Tung, O. Krupa, E. Apaydin, J.-J. Liou, A. Diaz-Santana, B. J. Kim and M. Wu, *Lab Chip*, 2013, **13**, 3876.
24 P. Vulto, P. Kuhn and G. A. Urban, *Lab Chip*, 2013, **13**, 2931.
25 P. Vulto, S. Podszun, P. Meyer, C. Hermann, A. Manz and G. A. Urban, *Lab Chip*, 2011, **11**, 1596.
26 K. A. Brakke, *Exp. Math.*, 1992, **1**, 141.
27 P. Concus and R. Finn, *Proc. Natl. Acad. Sci. U. S. A.*, 1969, **63**, 292.
28 A. Manz, N. Graber and H. M. Widmer, *Sens. Actuators, B*, 1990, **1**, 244.
29 S. Chibbaro, E. Costa, D. I. Dimitrov, F. Diotallevi, A. Milchev, D. Palmieri, G. Pontrelli and S. Succi, *Langmuir*, 2009, **25**, 12653.
30 T. S. Leu and P. Y. Chang, *Sens. Actuators, A*, 2004, **115**, 508.
31 J. Melin and S. R. Quake, *Annu. Rev. Biophys. Biomol. Struct.*, 2007, **36**, 213.
32 H. Bruus, *Theoretical Microfluidics*, Oxford University Press, New York, 2008, pp. 48–51.

